Journal of Luminescence 172 (2016) 92–98

Contents lists available at ScienceDirect

Journal of Luminescence

journal homepage: www.elsevier.com/locate/jlumin

Full Length Article

# Study of the Eosin-Y/PAMAM interactions in alkaline aqueous solution

Ernesto M. Arbeloa [a,b,*], Carlos M. Previtali [a,b], Sonia G. Bertolotti [a,b,*]

[a] Universidad Nacional de Río Cuarto, Río Cuarto, 5800 Córdoba, Argentina
[b] Consejo Nacional de Investigaciones Científicas y Técnicas (CONICET), Argentina

ARTICLE INFO

*Article history:*
Received 22 June 2015
Accepted 4 November 2015
Available online 8 December 2015

*Keywords:*
PAMAM dendrimers
Eosin-Y
Dye/dendrimer association
Host/guest system

ABSTRACT

The interactions between the xanthene dye Eosin-Y (Eos) and amino-terminated PAMAM dendrimers of low generations (G0–G3) were studied in alkaline water solution. The effect of concentration and generation of the dendrimer on the photophysics of Eos was evaluated by means of absorption and fluorescence spectroscopies. The observed spectral changes were ascribed to the association dye/dendrimer. From these data, the Eos/PAMAM binding constants ($K_{bind}$) were determined, which strongly increased with the size of the dendrimer. Stationary fluorescence anisotropy and time-resolved single photon counting were also used to characterize the association process. The restriction in the rotational diffusion of the Eos increased as a function of the concentration and generation of PAMAM, as determined by anisotropy measurements. Biexponential fluorescence decays were obtained in the presence of G3, and the respective lifetimes were ascribed to free and bound Eos species. These results correlate with $K_{bind}$ values and suggest the formation of host/guest system with larger dendrimers. Therefore, this environmentally-friendly dye/dendrimer system would be appropriate for potential applications in fields such as drugs delivery and photopolymerization.



## 1. Introduction

Supramolecular chemistry has expanded dramatically in recent years both in terms of potential applications and in its relevance to analogous biological systems. The formation and function of supramolecular complexes occur through a multiplicity of often difficult to differentiate noncovalent forces [1]. The structural characterization of these highly complex structures and their interaction mechanisms are ongoing challenges.

The development of molecular nanostructures with well-defined particle size and shape is of eminent interest in biomedical applications such as delivery of active pharmaceuticals, imaging, or gene transfection. For example, constructs utilized as carriers in drug delivery generally should be in the nanometer range and uniform in size to enhance their ability to cross cell membranes and to reduce the risk of undesired clearance from the body through liver or spleen [2].

Dendritic polymers or dendrimers provide an alternative route to create very well-defined nanostructures suitable for drug solubilization applications [3]. Dendrimers are core-shell nanostructures with precise architecture and low polydispersity, which are synthesized in a layer-by-layer fashion (expressed in 'generations') around a core unit, resulting in high level of control over size, branching points and surface functionality [2]. Dendrimers are highly branched and symmetrical macromolecules whose structures are well defined at nanoscale level [4]. The unique properties given by its particular architecture found applications in a wide variety of fields such as coatings, chemical sensors, catalytic nanoreactors and drug carriers among others [5–9]. Commercially available poly(amido amine) (PAMAM) and poly(propylene imine) (PPI or DAB) dendrimers have primary (peripheral) and tertiary (internal) amino groups, making them attractive for use in dye/amine photoinitiating systems of radical polymerizations. On this matter, a promising alternative to volatile and toxic amines are the amino-dendrimers. Some dye/amino-dendrimer systems have been characterized and applied in the initiation of radical polymerization [10–12]. However, this issue has not yet been fully explored and the reports are scarce.

On the other hand, combination of dendritic host with fluorescent guests gives rise to quenching/sensitization processes that can be exploited for a variety of purposes which include chemosensors, photon energy transfer, imaging, catalysis and elucidation of the intimate dendritic structure among other [13–16]. In this sense, Meijer and co-workers were pioneers in using dyes/dendrimers systems as host/guest models for drug delivery applications, from their so called "dendrimer box" [17,18].

Balzani et al. have found that the formation of host-guest species between xanthene dyes and peripherally functionalized poly(propylene imine) dendrimers, is related to the size of the

* Corresponding authors at: Universidad Nacional de Río Cuarto, Río Cuarto, 5800 Córdoba, Argentina.
*E-mail addresses:* earbeloa@exa.unrc.edu.ar (E.M. Arbeloa), sbertolotti@exa.unrc.edu.ar (S.G. Bertolotti).

http://dx.doi.org/10.1016/j.jlumin.2015.11.003
0022-2313/

macromolecule and to the electronic properties, rather than to the size of the dye molecule [19]. These authors founded that 12 Eosin-Y molecules can be hosted in the generation 5 and 25 molecules of Rose Bengal in the generation 4. On the other hand, Kline et al. were able to encapsulate and quantify multiple dyes in unmodified PAMAM dendrimers [20]. Selective uptake of dyes into dendrimers has also been observed by other researchers [21]. In this way, the dendrimers can be use potentiality for analytical applications, for example as extracting agents of dyes in water [22,23].

There are several reports that deal with the changes in photophysical properties of dyes due to its binding or encapsulating with dendrimers. For example, it has been reported that host/guest interactions modify the photophysical properties of Eosin and turn its monoexponential decay (typical of the aqueous solution) into a biexponential one in $CH_2Cl_2$ [24]. The existence of two lifetimes may be taken as an indication that there are two types or two families of sites in the dendrimer, or alternatively as a signal that there are two types of average interactions. Other authors used subnanosecond time-resolved techniques to assess the photophysics of Eosin-Y hosted into dansyl-modified PPI dendrimers [13,25,26]. They obtained several time-components in the order of the picoseconds that enabled elucidate the different energy transfer and relaxation processes. The ability to tune and modify the electronic properties of one or more guest molecules can be exploited practically, for instance in the field of light harvesting and chemical sensors.

Our group has been studying for over a decade the photophysics and photochemistry of dyes with electron donor or acceptor in both aqueous and microheterogeneous media [27–32]. In a previous work, we characterized the excited states of safranine dye in the presence of PAMAM and PPI dendrimers, in methanolic solution [33]. From absorption and emission spectra we concluded that this dye was not associated with the dendrimer and was preferably in the bulk of the solution. Quenching experiments demonstrated that amino dendrimers simply acts as a quencher by electron donation.

In this paper we characterized for the first time the photophysics of the xanthene dye Eosin-Y in the presence of amino-terminated PAMAM dendrimers in alkaline aqueous solution, an environment of low ecological impact. We decided to use commercially available dendrimers of low generations (G0–G3) without prior modifications. The effect of the dendrimer structure on the ground and excited singlet states was investigated by stationary and time-resolved spectroscopies. We have found that the dye was strongly associated with the dendrimers and the association constant correlated with the size of the host molecule. The results presented here about this dye/dendrimer system are relevant in order to assess its potential applications in any of the fields mentioned above.

## 2. Materials and methods

Eosin-Y and amino-terminated polyamido-amine (PAMAM) dendrimers of generations 0–3 (20% in methanol) were from Aldrich and used without further purification. Dendrimers solutions were properly diluted with HPLC grade methanol (Sintorgan) as necessary. Water solutions were prepared with bi-distilled water. The pH of the solutions was adjusted by analytical grade NaOH.

Absorption spectra were recorded on a Hewlett Packard 6453E diode array spectrophotometer. Emission spectra and fluorescence anisotropy were measured with a Horiba Jobin Yvon FluoroMax-4 spectrofluorometer. Time-correlated single photon counting experiments were performed on a FL 900 Edinburgh Instruments equipped with a $H_2$ lamp. Excitation wavelength was fixed at 517 nm and emission was monitored at 536 nm. A 1-cm-pathlength quartz cuvette was used in all spectroscopic assays.

The concentrations of the alkaline aqueous solutions of Eos were 3–6 μM (Abs ~ 0.3–0.6 at 517 nm) in absorption measurements and the absorbance of the solutions was adjusted to ~0.05 at excitation wavelength for emission experiments. Throughout all experiments the addition of the dendrimers was performed by microsyringes under constant stirring, such that the methanol content in the Eos solutions was < 5%. There were no changes in the spectra by this additional methanol, as verified through blank tests. All data were properly corrected by dilution effects. The measurements were performed at least by duplicate.

## 3. Results and discussion

The ground and singlet excited states of Eos in the absence and presence of amino-terminated PAMAM dendrimers of generations 0–3 (G0–G3) were characterized in alkaline aqueous solution (pH 9.5), by means of spectroscopic measurements. Solutions of the dye alone registered an absorption maximum at 517 nm and the emission spectra showed a broad band centered at 536 nm, in good agreement with reported values [34,35]. However, changes in the position and intensity of the spectral bands were observed in the presence of the dendrimers. In Fig. 1 are shown the absorption spectra of Eos with different PAMAM concentrations. A progressive bathochromic shift is observed with the increase in the content of each dendrimer. Moreover, the intensity of the absorption maximum decreased with the addition of PAMAM. These changes were most noticeable as the dendrimer generation was higher.

As it has been reported, Eos shows a red shift in the absorption and emission bands as solvent polarity decreases [27,34,35]. Also, some studies with fluorescent probes have demonstrated that the internal cavities of PPI and PAMAM dendrimers are significantly less polar than water [36–38]. A red shift in the absorption and emission spectra of Eos hosted into a peripherally modified PPI dendrimer in non-aqueous solvents has been reported by others [13,19,24,25]. They observed an absorption maximum at *ca.* 530 nm when the dye was associated into PPI from generations 3 to 5 [19,25]. Fig. 1 shows that the absorption maximum of Eos is shifted from 517 in pure alkaline water to 526 nm in the presence of G3. These results are similar to those reported for the dye in the presence of the cationic surfactant CTAB in aqueous solution [35]. It has been reported that polarity of the CTAB/water interface is similar to n-alcohols [39], and we registered a maximum wavelength of 527 nm for Eos in 1-propanol (data not shown). Therefore, the spectroscopic changes observed in the presence of PAMAM dendrimers may be due to Eos is sensing a less polar environment than in aqueous solution. All data suggest that Eos is binding with the dendrimers in a size-dependent way. Moreover, the occurrence of an isosbestic point in the Fig. 1 evidences the presence of two species in equilibrium, which could be ascribed to the free and dendrimer-associated Eos.

Fig. 2 shows the fluorescence spectra of the dye in the presence of PAMAM dendrimers. It can be seen a progressive emission quenching when the dendrimer concentration is increased for all generations assessed. The quenching and red shifts increase on going from G0 to G3; however, minor bathochromic shifts are observed.

From data of fluorescence intensity at 536 nm (Fig. 2), the Stern–Volmer plots were constructed and showed a downward curvature for all generations of PAMAM used (Fig. 3). Estimative values of the Stern–Volmer constant ($K_{SV}$) may be obtained, by fitting the initial points to straight lines (Table 1). From $K_{SV}$ values

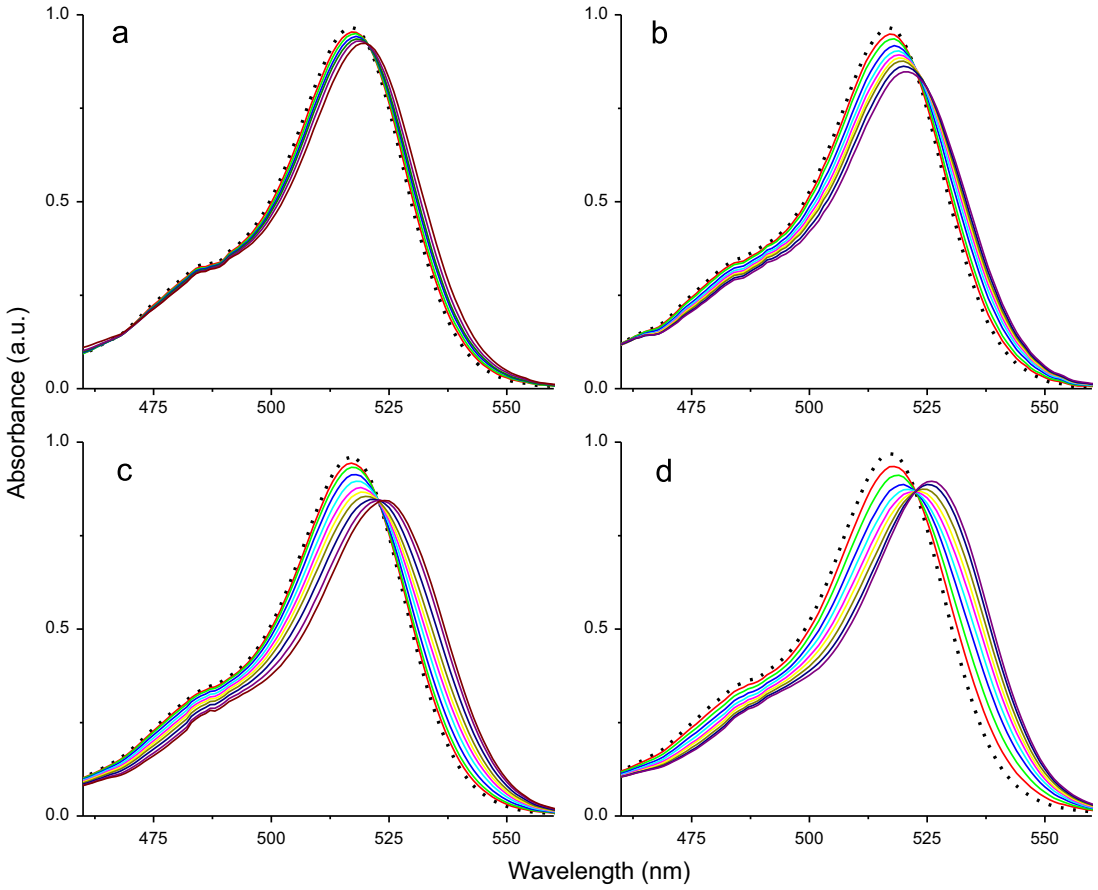


**Fig. 1.** Absorption spectra of Eos in alkaline aqueous solution in the absence (−), and in the presence of PAMAM dendrimers: a) 1.6–15.7 mM of G0; b) 0.14–3.0 mM of G1; c) 0.03–2.0 mM of G2; d) 0.01–0.48 mM of G3. The concentration of PAMAM increases from left to right.

and the observed singlet-state lifetime of Eos in water (1.15 ns), the apparent quenching rate constants ($^1$kq) were much larger than diffusion-controlled limit in water ($k_{diff}=7.4\times10^9$ M$^{-1}$ s$^{-1}$, at 25 °C, [40]) for all dendrimers assayed. This implies that the observed decrease in fluorescence intensity is not occurring by a collisional quenching process. A plausible explanation is that close proximity between Eos molecules and more than one amino groups on the dendrimer promoted by the strong association, might account for the so high $^1$kq registered. Such interpretation has been proposed by others to explain $^1$kq values longer than $k_{diff}$ reported for dye/protein associations [41,42].

The downward deviation from linearity observed in Fig. 3 might be ascribed to two main causes: i) the residual fluorescence from Eos associated to the dendrimer or ii) the occurrence of more than one type of binding sites in the macromolecule [43]. However, the last cause can be discarded because the downward curvature was also registered in the presence of G0. This small dendrimer has a completely open structure free from internal cavities, and therefore it cannot have more than one type of binding site. Extrapolating this argument to other generations used, we may ascribe the deviation from linearity to the residual emission. Balzani et al. [19,24] also reported a residual emission for Eos hosted into a series peripherally modified PPI dendrimers. A more noticeable confinement effect on fluorescence properties was also registered for the structurally-related xanthene dye Rose Bengal, hosted into PPI-G5 dendrimer [18]. In the presence of the dendrimer this dye showed an intense fluorescence band, which is completely absent in water solution.

In order to characterize the extent of the Eos/dendrimer association, the corresponding binding constants ($K_{bind}$) were determined. Absorption and fluorescence data were used independently to verify the reliability of the results.

From a simple equilibrium model between Eos and dendrimer, a 1:1 stoichiometry for Eos/dendrimer complex (EosD) may be considered (Eqs. (1) and (2)). This assumption is reasonable because the dendrimer concentration was at least 200-fold greater than that of Eos for all generations used, which gives a very low probability of obtaining a binding ratio Eos/D > 1. Also, equivalent and independent sites were assumed. The same assumptions have been made by other authors to determine $K_{bind}$ values of PAMAM with several drugs [44,45].

$$Eos_f + D_f \leftrightarrow EosD \tag{1}$$

$$K_{bind} = \frac{[EosD]}{[Eos_f][D_f]} \tag{2}$$

where $Eos_f$ and $D_f$ stand for free Eos and dendrimer molecules, respectively.

The observed absorbance in the 450–600 nm range only depends on Eos concentration (both, in its free and associated forms), since PAMAM dendrimers do not absorb in the visible region:

$$A = A_{free} + A_{bind} = \epsilon_f[Eos_f] + \epsilon_{bind}[EosD] \tag{3}$$

where $\varepsilon_f$ and $\varepsilon_{bind}$ stands for molar extinction coefficients of free and associated Eos, respectively. Considering Eqs. (2) and (3) and the respective masses balances, next expression for the absorbance may be deduced:

$$A - Ao = \frac{[Eos]K_{bind}\Delta\epsilon[D]}{1+K_{bind}[D]} \tag{4}$$

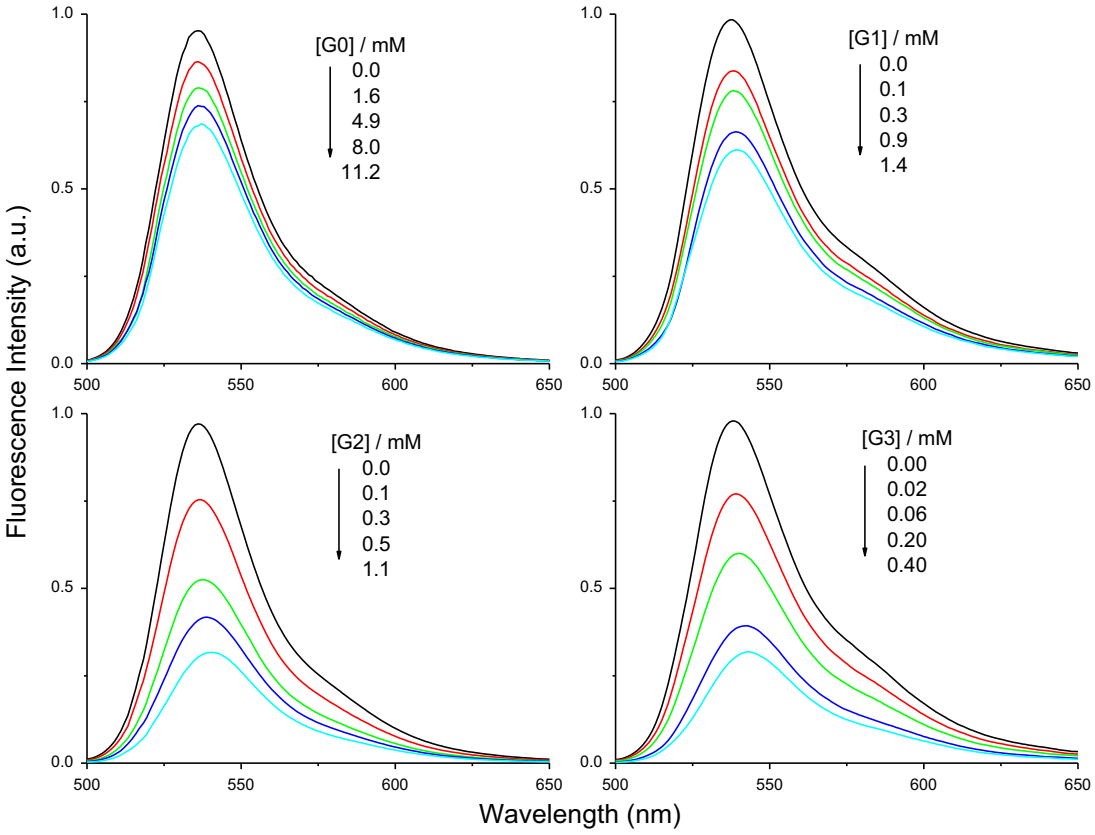


**Fig. 2.** Fluorescence spectra of Eos in alkaline aqueous solution as a function of concentration and generation of PAMAM.

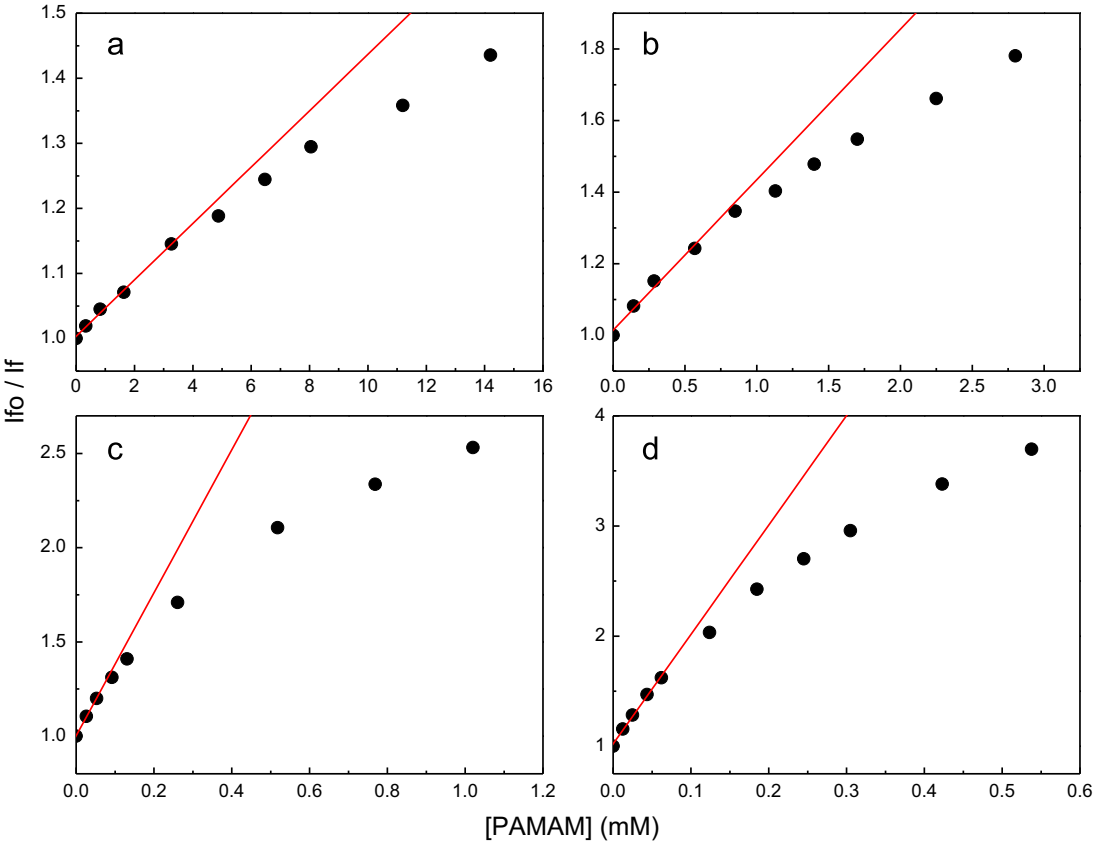


**Fig. 3.** Stern–Volmer plots at 536 nm for Eos in the presence of PAMAM dendrimers: a) G0; b) G1; c) G2 and d) G3.

Here *Ao* is the absorbance in the absence of dendrimer; and $\Delta\varepsilon$ is the difference between $\varepsilon_{bind}$ and $\varepsilon_f$. Note that in this equation $[D_f]$ has been replaced by [D], the total dendrimer concentration. This approximation is reasonable because of the excess of dendrimer used. Eq. (4) may be rearranged at a linearized expression as follows:

$$\frac{1}{\Delta A}=\frac{1}{[Eos]K_{bind}\Delta\epsilon[D]}+\frac{1}{[Eos]\Delta\epsilon} \quad (5)$$

According to Eq. (5), at fixed Eos concentration a double reciprocal plot of $1/\Delta A$ vs. 1/[D] should fit to straight line and $K_{bind}$ can be estimated from the intercept/slope ratio. Also, from the respective intercepts the values of $\varepsilon_{bind}$ at a given wavelength may be determined.

Alternatively, $K_{bind}$ can be expressed in terms of the fraction ($\alpha$) of Eos molecules that are bound to the dendrimer (Eq. (6)). In an equivalent and independent sites model, $\alpha$ can be expressed in terms of the fluorescence intensity as follows [43]:

$$K_{bind}=\frac{\alpha}{(1-\alpha)[D_T]} \quad (6)$$

**Table 1**
Stern–Volmer constant ($K_{SV}$) for Eos in the presence of PAMAM dendrimers.

| Quencher | $K_{SV}$ ($M^{-1}$) |
|---|---|
| G0 | 45 |
| G1 | 515 |
| G2 | 3140 |
| G3 | 9860 |

$$\alpha=\frac{Fo-F}{Fo-F^*} \quad (7)$$

where *Fo* and *F* stand for fluorescence intensity at fixed wavelength in the absence and presence of dendrimer, respectively. As mentioned these dendrimers do not absorb at excitation wavelength, whereby the emission recorded correspond to Eos molecules. $F^*$ is the residual emission extrapolated at infinite saturation, *i.e.* when hypothetically all Eos would be bonded to dendrimer. Therefore, $F^*\neq 0$ would indicate an emission from EosD complex formed.

From Eqs. (6) and (7), a similar expression as Eq. (4) may be derived for emission measurements:

$$Fo-F=\frac{K_{bind}[D](Fo-F^*)}{1+K_{bind}[D]} \quad (8)$$

It can be demonstrated that in absence of residual emission ($F^*=0$), Eq. (8) reduces to Stern–Volmer equation with $K_{bind}\equiv K_{SV}$ [46]. Again, Eq. (8) can be linearized to obtain another expression analogous to Eq. (5):

$$\frac{1}{\Delta F}=\frac{1}{K_{bind}[D](Fo-F^*)}+\frac{1}{(Fo-F^*)} \quad (9)$$

From Eq. (9), a plot of $1/\Delta F$ vs. 1/[D] should fit a straight line, which enables calculate $K_{bind}$ from its intercept/slope ratio.

As an example, in the Fig. 4 are shown the plots according to Eq. (5) for all generations of PAMAM analyzed. Each plot fits very well to a straight line (regression coefficient $R>0.9900$), which validates the assumptions in the model proposed. Similar plots were obtained from fluorescence data (not shown for simplicity). The corresponding $K_{bind}$, $\varepsilon_{bind}$ and residual fluorescence values are summarized on Table 2.

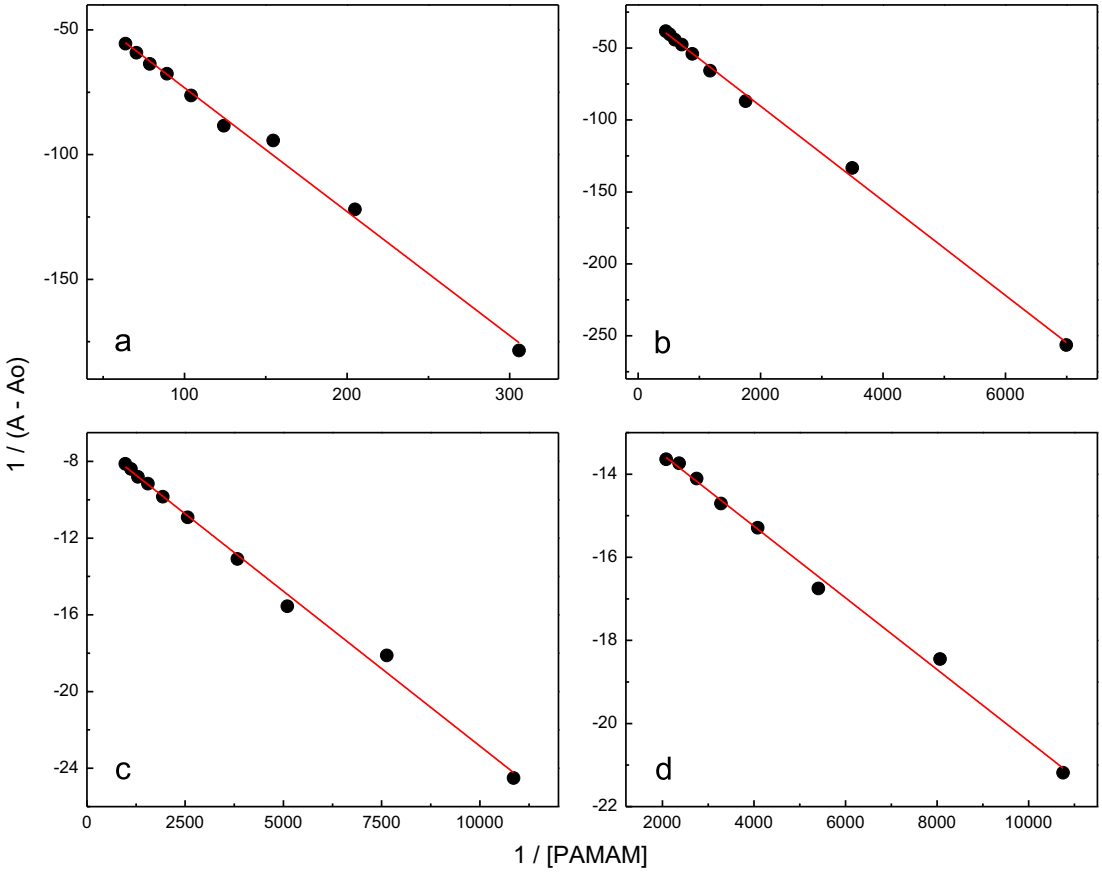


**Fig. 4.** Plots of $1/\Delta A$ vs. 1/[D] according to Eq. (5) for Eos in the presence of PAMAM dendrimers: a) G0; b) G1; c) G2 and d) G3.

**Table 2**
Binding constants ($K_{bind}$), absorptivity-molar coefficients at 517 nm ($\varepsilon^{517}_{bind}$) and residual fluorescence (F*/Fo) for the Eos/PAMAM complexes in alkaline aqueous solution.

| Eos species | $K_{bind}$ ($M^{-1}$)[a] | | $\varepsilon^{517}_{bind}$ ($M^{-1}$ $cm^{-1}$)[a] | F*/Fo |
|---|---|---|---|---|
| | Absorption | Fluorescence | | |
| Eos | – | – | 90700[b] | – |
| Eos/G0 | 50 | 95 | 77900 | 0.53 |
| Eos/G1 | 780 | 1160 | 78200 | 0.41 |
| Eos/G2 | 5800 | 5600 | 71500 | 0.33 |
| Eos/G3 | 12900 | 14700 | 68400 | 0.19 |

[a] Estimated error ± 10%.
[b] Value in alkaline water ($\varepsilon_f$) obtained by means of Lambert-Beer treatment.

As expected from spectra in Fig. 1, the $\varepsilon_{bind}$ values at 517 nm obtained from Eq. (5) decreased as compared to that of $\varepsilon_f$. Within the experimental error, it can distinguish two values for $\varepsilon_{bind}$: for smaller generations (*i.e.* G0 and G1) the $\varepsilon_{bind}$ were around 80000 $M^{-1}$ $cm^{-1}$, whereas for larger ones (*i.e.* G2 and G3) were around 70000 $M^{-1}$ $cm^{-1}$. A comparable decrease in the value of $\varepsilon$ was observed for Eos hosted into PPI dendrimers [19]. The authors reported a maximum value of 60000 $M^{-1}$ $cm^{-1}$ for totally encapsulated Eos. The similitude between this value and those reported on Table 2 for Eos/G2 and Eos/G3 complexes suggests that Eos might be hosted into the larger PAMAM dendrimers, at least partially.

According to Eq. (9) the residual emission gradually decreased with the size of the dendrimer (denoted as the *F*/Fo* ratio on Table 2). Moreover, the higher $K_{SV}$, the lower *F*/Fo* ratio (compare to data on Table 1). This indicates that a more effective quenching process is occurring, probably because Eos is being surrounded by an increasing local concentration of tertiary amino groups. Similar tendency on residual emission was reported for Eos hosted into PPI dendrimers [19].

The hypothesis about the host-guest complex formation between Eos and PAMAM in the present experimental conditions is also supported by the values of $K_{bind}$ obtained. Table 2 shows that there is a strong dependence on the values of $K_{bind}$ with the size of the dendrimer, which increments up three orders of magnitude from G0 to G3. Importantly, values of $K_{bind}$ were mutually consistent for both spectroscopic techniques used, thus validating the reliability of the results. Because of the small size of the G0 and G1, the association dye/PAMAM only can be superficial. However, the simple association of Eos to the outer surface of the larger PAMAM (G2 and G3) would not explain such notorious increment in the $K_{bind}$ values.

The singlet-state decay kinetics of Eos in alkaline aqueous solutions in the absence and the presence of PAMAM dendrimers were obtained by time-resolved single photon counting (TR-SPC) experiments. In the absence of PAMAM Eos showed monoexponential emission decay with a lifetime of $1.2 \pm 0.1$ ns in agreement with reported values [34,47]. The dendrimer concentration ranges used for these measurements (*ca.* 5–14 mM for G0 and *ca.* 0.1–0.5 mM for G3) correspond to those of the downward curvature in the Stern–Volmer plots (Fig. 3). In the presence of G0, monoexponential decays were also registered and the lifetimes obtained were similar to that of Eos in aqueous solution. Therefore, the ratio $\tau_o/\tau \approx 1$ indicates that a static quenching process is occurring.

On the other hand, the singlet-state decay kinetics of Eos in the presence of G3 were biexponential. A time distribution analysis showed a major component of *ca.* 1 ns and a minor component (less than 5% of the total emission) of *ca.* 2-3 ns for the whole concentration range of dendrimer used. According to emission spectra (Fig. 2), the shorter time may be ascribed to the free unquenched Eos in the bulk aqueous solution. The longer time might be ascribed to Eos hosted into dendrimer, which would be sensing a microenvironment less polar than water ($\tau \approx 3$ ns in ethanol, [34,48]). Similar lifetime values were reported for Eos hosted in G2–G4 peripherally modified PPI dendrimers [19,24,48]. Although our experimental conditions (type and generation of the dendrimer, dye/dendrimer ratios) and the characteristics of our TR-SPC equipment (time-scale and sensitivity) were different than used in those reports, our results agree with those of the authors.

In order to gain more insights about nature of dye/dendrimer association, the steady-state emission anisotropy of Eos in the presence of PAMAM was analyzed. Anisotropy describes the extent of emission polarization caused by, mostly, restrictions in rotational diffusion of a particular fluorophore. Increases in steady-state anisotropy values are generally observed with increasing rigidity in the microenvironment of such fluorophore, since a more rigid confinement hinders rotational diffusion. In order to gain more insights about the surroundings that Eos senses in the presence of PAMAM dendrimers, emission anisotropy experiments were conducted. A progressive increment in anisotropy signal was recorded, as the concentration of dendrimer was increased (Fig. 5). Further, Fig. 5 shows a more drastic raise in anisotropy as a function of dendrimer generation, from G0 to G3. The concentration effect observed seems to indicate that the environment restrictions increased as more Eos/D complex was generated. In turn, in the presence of larger dendrimers the Eos may be surrounded more closely by the macromolecule or even be entrapped therein. It is known that from generations 2-3 PAMAM structures begin to become more globular in solution [4]. Other authors have reported similar trends on steady-state anisotropy of dyes as a function of the dendrimer generation [20,37,49]. Although their results were indicative of the dye–dendrimer association, the main contribution to anisotropy was ascribed to molecular volume increase with dendrimer generation. However, they worked at fixed dendrimer concentration of $10^{-4}$ M, which is very high compared to that we used for larger generations (Fig. 5). It would not be surprising that the drastic change here observed in the anisotropy of the largest generations is due to the formation of a host/guest complex. Indeed, the differences in $K_{bind}$ values according to Table 1 support this hypothesis.

## 4. Conclusions

The effect of PAMAM dendrimers G0–G3 on the photophysical parameters of Eos provides strong evidence that the dye associates whit the dendrimers, even with those of the lower generation. The extent of this association increased significantly with the size of the macromolecule, as it may be seen from the $K_{bind}$ values obtained. These findings suggest that there is only a surface association between Eos and the lowest generations of PAMAM, whereas for more structurally-globular dendrimers assessed here a host/guest system formation is probable. The data from TR-SPC and fluorescence anisotropy strongly support this hypothesis.

The results obtained in the present work encourage us to further study of the Eos/PAMAM systems in order to apply it in both, the initiation of vinyl polymerizations and the drugs delivery. In particular, we are undertaking a more complete characterization of the Eos triplet state in the presence of PAMAM dendrimers. We expect a high efficiency in the formation of reactive radicals because the strong association Eos/PAMAM allows the close proximity between the dye and several electron-donor amino groups. Furthermore, the aqueous complex evaluated here present a very low ecological impact versus the photoinitiating systems based on organic solvents and volatile amines.

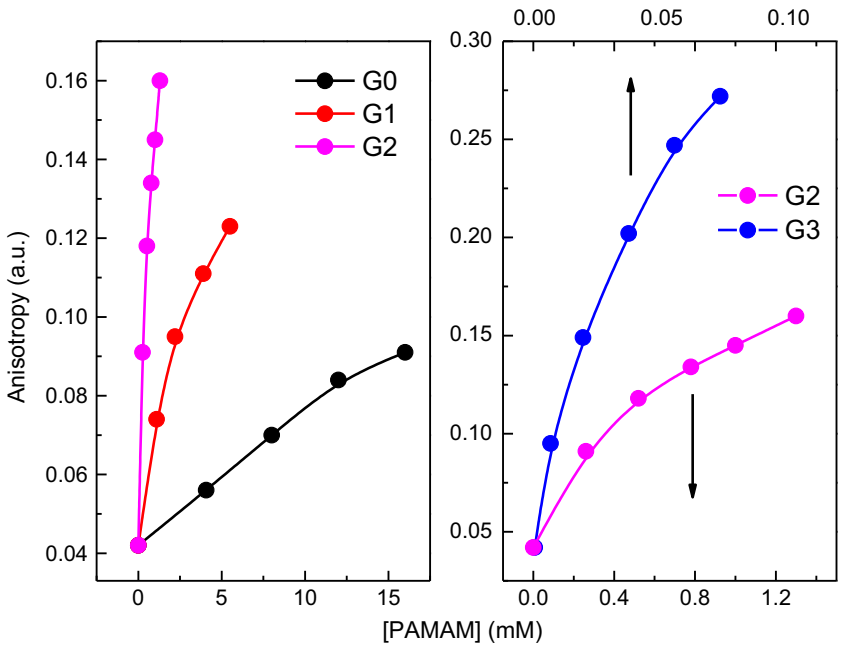


**Fig. 5.** Fluorescence anisotropy of Eos as a function of concentration and generation of PAMAM dendrimers.

## Acknowledgments

Financial support from the Agencia Nacional de Promoción Científica y Tecnológica (PICT: 1224/2013), CONICET (PIP: 2010-0284) and Universidad Nacional de Río Cuarto is gratefully acknowledged.

## References

[1] H.-J. Schneider, Angew. Chem. Int. Ed. 48 (2009) 3924.
[2] S. Svenson, Eur. J. Pharm. Biopharm. 71 (2009) 445.
[3] S. Mignani, S.E. Kazzouli, M. Bousmina, J.-P. Majoral, Prog. Poly. Sci. 38 (2013) 993.
[4] D.A. Tomalia, A.M. Naylor, W.A. Goddard, Angew. Chem. Int. Ed. Engl. 29 (1990) 138.
[5] D. Astruc, Nat. Chem. 4 (2012) 255.
[6] D. Astruc, E. Boisselier, C. Ornelas, Chem. Rev. 110 (2010) 1857.
[7] Y. Cheng, L. Zhao, Y. Li, T. Xu, Chem. Soc. Rev. 40 (2011) 2673.
[8] P. Kesharwani, K. Jain, N.K. Jain, Prog. Polym. Sci. 39 (2014) 268.
[9] S. Svenson, D.A. Tomalia, Adv. Drug. Deliv. Rev. 64 (2012) 102.
[10] X. Jiang, J. Yin, Macromolecules 37 (2004) 7850.
[11] X. Jiang, W. Wang, H. Xu, J. Yin, J. Photochem. Photobiol. A: Chem. 181 (2006) 233.
[12] M.A. Tasdelen, A.L. Demirel, Y. Yagci, Eur. Polym. J. 43 (2007) 4423.
[13] J. Aumanen, J. Korppi-Tommola, Chem. Phys. Lett. 518 (2011) 87.
[14] J. Han, C. Gao, Curr. Org. Chem. 15 (2011) 2.
[15] K.K. Kline, S.A. Tucker, J. Phys. Chem. A 114 (2010) 7338.
[16] C.A. Dougherty, J.C. Furgal, M.A. van Dongen, T. Goodson 3rd, M.M. Banaszak Holl, J. Manono, S. DiMaggio, Chem. Eur. J. 20 (2014) 4638.
[17] J.F.G.A. Jansen, E.W. Meijer, E.M.M. de Brabander-van den Berg, J. Am. Chem. Soc. 117 (1995) 4417.
[18] J.F.G.A. Jansen, E.W. Meijer, E.M.M. De Brabander - Van Den Berg, Macromol. Symp. 102 (1996) 27.
[19] V. Balzani, P. Ceroni, S. Gestermann, M. Gorka, C. Kauffmann, F. Vögtle, Tetrahedron 58 (2002) 629.
[20] K.K. Kline, E.J. Morgan, L.K. Norton, S.A. Tucker, Talanta 78 (2009) 1489.
[21] E.J. Morgan, J.M. Rippey, S.A. Tucker, Appl. Spectrosc. 60 (2006) 551.
[22] M.W.P.L. Baars, E.W. Meijer, P.E. Froehling, Chem. Commun. 20 (1997) 1959.
[23] N.M. Mahmoodi, B. Hayati, M. Arami, F. Mazaheri, J. Chem. Eng. Data 55 (2010) 4660.
[24] V. Balzani, P. Ceroni, S. Gestermann, M. Gorka, C. Kauffmann, M. Maestri, F. Vogtle, Chem. Phys Chem 1 (2000) 224.
[25] J. Aumanen, V. Lehtovuori, N. Werner, G. Richardt, J. van Heyst, F. Vögtle, J. Korppi-Tommola, Chem. Phys. Lett. 433 (2006) 75.
[26] J. Aumanen, T. Kesti, V. Sundstrom, G. Teobaldi, F. Zerbetto, N. Werner, G. Richardt, J. van Heyst, F. Vogtle, J. Korppi-Tommola, J. Phys. Chem. B 114 (2010) 1548.
[27] E.M. Arbeloa, G.V. Porcal, S.G. Bertolotti, C.M. Previtali, J. Photochem. Photobiol. A: Chem. 252 (2013) 31.
[28] G.V. Porcal, M.S. Altamirano, S.G. Bertolotti, C.M. Previtali, J. Photochem. Photobiol. A: Chem. 219 (2011) 62.
[29] G.V. Porcal, M.S. Altamirano, C.A. Glusko, S.G. Bertolotti, C.M. Previtali, Dyes Pigment. 88 (2011) 240.
[30] G.V. Porcal, E.M. Arbeloa, D.E. Orallo, S.G. Bertolotti, C.M. Previtali, J. Photochem. Photobiol. A: Chem. 226 (2011) 51.
[31] G.V. Porcal, C.A. Chesta, M.A. Biasutti, S.G. Bertolotti, C.M. Previtali, Photochem. Photobiol. Sci. 11 (2012) 302.
[32] G.V. Porcal, C.M. Previtali, S.G. Bertolotti, Dyes Pigment. 80 (2009) 206.
[33] C.A. Suchetti, A.I. Novaira, S.G. Bertolotti, C.M. Previtali, J. Photochem. Photobiol. A: Chem. 201 (2009) 69.
[34] G.R. Fleming, A.W.E. Knight, J.M. Morris, R.J.S. Morrison, G.W. Robinson, J. Am. Chem. Soc. 99 (1977) 4306.
[35] M. Chakraborty, A.K. Panda, Spectrochim. Acta A: Mol. Biomol. Spectrosc. 81 (2011) 458.
[36] G. Pistolis, A. Malliaris, C.M. Paleos, D. Tsiourvas, Langmuir 13 (1997) 5870.
[37] D.L. Richter-Egger, J.C. Landry, A. Tesfai, S.A. Tucker, J. Phys. Chem. A 105 (2001) 6826.
[38] G. Pistolis, A. Malliaris, Langmuir 18 (2002) 246.
[39] K.A. Zachariasse, P. Nguyen Van, B. Kozankiewicz, J. Phys. Chem. 85 (1981) 2676.
[40] D.R. Lide, CRC Handbook of Chemistry and Physics, 84th ed., CRC Press, Boca Raton, FL, 2003.
[41] E. Alarcon, A.M. Edwards, A. Aspee, C.D. Borsarelli, E.A. Lissi, Photochem. Photobiol. Sci. 8 (2009) 933.
[42] E. Alarcon, A.M. Edwards, A. Aspee, F.E. Moran, C.D. Borsarelli, E.A. Lissi, D. Gonzalez-Nilo, H. Poblete, J.C. Scaiano, Photochem. Photobiol. Sci. 9 (2010) 93.
[43] E. Alarcon, A. Aspee, E.B. Abuin, E.A. Lissi, J. Photochem. Photobiol. B: Biol. 106 (2012) 1.
[44] A. Abderrezak, P. Bourassa, J.-S. Mandeville, R. Sedaghat-Herati, H.-A. Tajmir-Riahi, PloS One 7 (2012) e33102.
[45] J.S. Hansen, M. Ficker, J.F. Petersen, B.E. Nielsen, S. Gohar, J.B. Christensen, J. Phys. Chem. B 117 (2013) 14865.
[46] M. van de Weert, L. Stella, J. Mol. Struct. 998 (2011) 144.
[47] M.V. Encinas, A.M. Rufs, S.G. Bertolotti, C.M. Previtali, Polymer 50 (2009) 2762.
[48] J. Aumanen, G. Teobaldi, F. Zerbetto, J. Korppi-Tommola, RSC Adv. 1 (2011) 1778.
[49] D.L. Richter-Egger, A. Tesfai, S.A. Tucker, Anal. Chem. 73 (2001) 5743.